

# Area Selective Deposition of Metals from the Electrical Resistivity of the Substrate

*Hama Nadhom, Robert Boyd, Polla Rouf, Daniel Lundin, and Henrik Pedersen\**

*Department of Physics, Chemistry and Biology, Linköping University, SE-58183 Linköping, Sweden*

*\*Corresponding author, e-mail: henrik.pedersen@liu.se*

## ABSTRACT

Area selective deposition (ASD) of films only on desired areas of the substrate opens for less complex fabrication of nanoscaled electronics. We show that a newly developed CVD method, where plasma electrons are used as the reducing agent in deposition of metallic thin films, is inherently area selective from the electrical resistivity of the substrate surface. When depositing iron with the new CVD method, no film is deposited on high-resistivity SiO<sub>2</sub> surfaces whereas several hundred nm thick iron films are deposited on areas with low resistivity, obtained by adding a thin layer of silver on the SiO<sub>2</sub> surface. Based on such a scheme, we show how to use the electric resistivity of the substrate surface as an extension of the ASD toolbox for metal-on-metal deposition.

Miniaturization of electronic components has increased the demand for precise and improved thin film deposition methods. For example, deposition only on desired areas would avoid the need for patterning and etching steps and allow for bottom-up fabrication of nano scaled structures. This has motivated research into area selective deposition (ASD) by chemical vapor deposition (CVD) techniques.<sup>1,2,3</sup> The selectivity in ASD is usually achieved by changing the surface chemistry of either the area where film growth is desired or not desired to control the adsorption of precursor molecules to only specific areas on the substrate. Different methods have been reported to enable ASD. Self-assembled monolayers of organic molecules are often used to block areas of the surface where no film growth is desired.<sup>4</sup> Film nucleation can also be inhibited on certain areas on the surface by surface passivation using ion implantation or by small inhibitor molecules such as fluorine, hydrogen or ammonia.<sup>5,6,7</sup> ASD can also be achieved by utilizing different film growth rate or nucleation rates on different materials on the substrate.<sup>8</sup> This approach can be further enhanced by adding etching steps to the deposition process.<sup>9</sup>

We recently reported a new CVD method for deposition of metallic films where the free electrons in a plasma are used as reducing agents.<sup>10</sup> Since the method draws an electron current from the plasma to an electrically biased substrate, a conducting surface is needed to close the electric circuit allowing the electron current to flow from the plasma discharge to the bias power supply without any charge build-up. Therefore, metallic films could be deposited on electrically conducting silver substrates, whilst the deposition process was hampered on poorly conductive silicon and inactive on insulating silicon dioxide substrates. Here, we show how this inherent surface selectivity can be used to afford an area selective deposition of metallic thin films on only areas of a substrate surface that are electrically conducting.

Iron films were deposited from ferrocene, bis(cyclopentadienyl)Fe(II) (FeCp<sub>2</sub>), with plasma electrons as reducing agents on a 1 × 2 cm<sup>2</sup> Si (100) substrate with a 300 nm thermally

grown SiO<sub>2</sub> layer, partially covered by a 40 nm thick layer of sputter coated silver. The deposition system setup and the experimental procedures of our new CVD method are described elsewhere.<sup>10</sup> Briefly, the depositions were carried out in a vacuum chamber equipped with a hollow cathode plasma source located in the top lid of the vacuum chamber. Argon was used as working gas at a flow rate of 70 sccm through the titanium hollow cathode. The plasma discharge was maintained at 70 W in DC mode at a working gas pressure of 25 Pa. FeCp<sub>2</sub> was supplied by evaporation at 70 °C and the vapor was drawn into the deposition chamber by the chamber vacuum. The stainless-steel substrate holder (65 × 42 × 1 mm) was placed in the precursor stream, upstream from the plasma source to allow precursors to adsorb on the substrate without entering the plasma bulk to minimize plasma chemical decomposition of the metal precursors. A DC bias voltage of 40 V, connected to the steel sample holder, was used to attract the plasma electrons to the substrate. Drawing an electronic current resulted in a slight heating of the substrate holder and a temperature of 40 °C was measured by a thermocouple spot-welded to the backside of the substrate holder. This was regarded as the deposition temperature as no other heating was used. The substrates were electrically connected to the substrate holder using silver paint on both the silver coated and the SiO<sub>2</sub> sides of the substrate. The deposition time was 60 s.

Cross section scanning transmission electron microscopy (STEM) was used to determine the presence, thickness and chemical structure of the deposited films. Prior to analysis, thin sections suitable for analysis by STEM were prepared using the lift out approach based on focused ion beam milling.<sup>11</sup> All STEM analysis were performed using a FEI Tecnai G2 TF 20 UT instrument operated at 200 kV. Images were collected with an annular detector spanning the range 80 to 260 mrad. The composition of the deposited films layers was determined by energy dispersive X-ray spectroscopy (EDS) analysis and elemental mapping.

X-ray photoelectron spectroscopy (XPS) was used to analyze the elemental composition and chemical bonding in the deposited films using monochromatic Al K $\alpha$  X-rays. A charge neutralizer filament was used to compensate for the charge build-up effect. The conditions used for survey scans were as follows: energy range = 0–1200 eV, pass energy = 160 eV, step size = 0.1 eV, and X-ray spot size = 2 mm in diameter. A binding energy range of 20–40 eV (depending on the examined peak) was used for high-resolution spectra with a pass energy of 20 eV. Argon (0.5 keV) was used as the sputtering source. The C 1s peak with a value of 285 eV was used for calibration in all spectra. Gaussian–Laurentius (GL) functions and a Shirley back-ground were used to fit the experimental XPS data.

Cross section STEM analysis (Figure 1) shows that an approximately 400 nm thick film is deposited on the Ag coated areas of the SiO $_2$  (resistivity  $\rho_{\text{Ag,bulk}} = 1.59 \times 10^{-8} \Omega\text{m}$ )<sup>12</sup> (Figure 1a), while no film can be seen on the bare SiO $_2$  (resistivity  $\rho_{\text{Silica}} = 5 \times 10^{11}–10^{14} \Omega\text{m}$ )<sup>12</sup> (Figure. 1b). The deposited Fe film is relatively rough, with height variations of 100 nm and porous, which is more prevalent near the Ag layer. Compositional mapping by STEM-EDS (inserts in Figure 1a and 1b), reveals that the film deposited on Ag coated is Fe rich. Further analysis of the EDS data shows that the film also has a high O content (composition FeO $_{1.3}$ ) with trace amounts of Ti and C. The presence of Ti is most likely due to sputtering of the titanium hollow cathode and the presence of C is in part due to contamination during preparation and analysis. This indicates that the analyzed films have a high concentration of iron oxide, due to the porous nature of the film (Figure 1), a significant portion of which could have been formed when the newly revealed Fe was exposed to air. The selected area electron diffraction of the iron film shows no diffraction spots and HRTEM analysis of the film could not resolve any diffraction fringes (data not shown). Both of which indicates that the film is amorphous when analyzed. The TEM analysis of the substrate areas not coated by Ag show no film growth and no iron could be detected by EDS. From the TEM analysis it is seen that the silicon oxide material has

a very rough morphology with height variations of 50 nm. We ascribe this to etching by the plasma–surface interactions when the deposition process attempts to draw a current of plasma electrons through the surface.

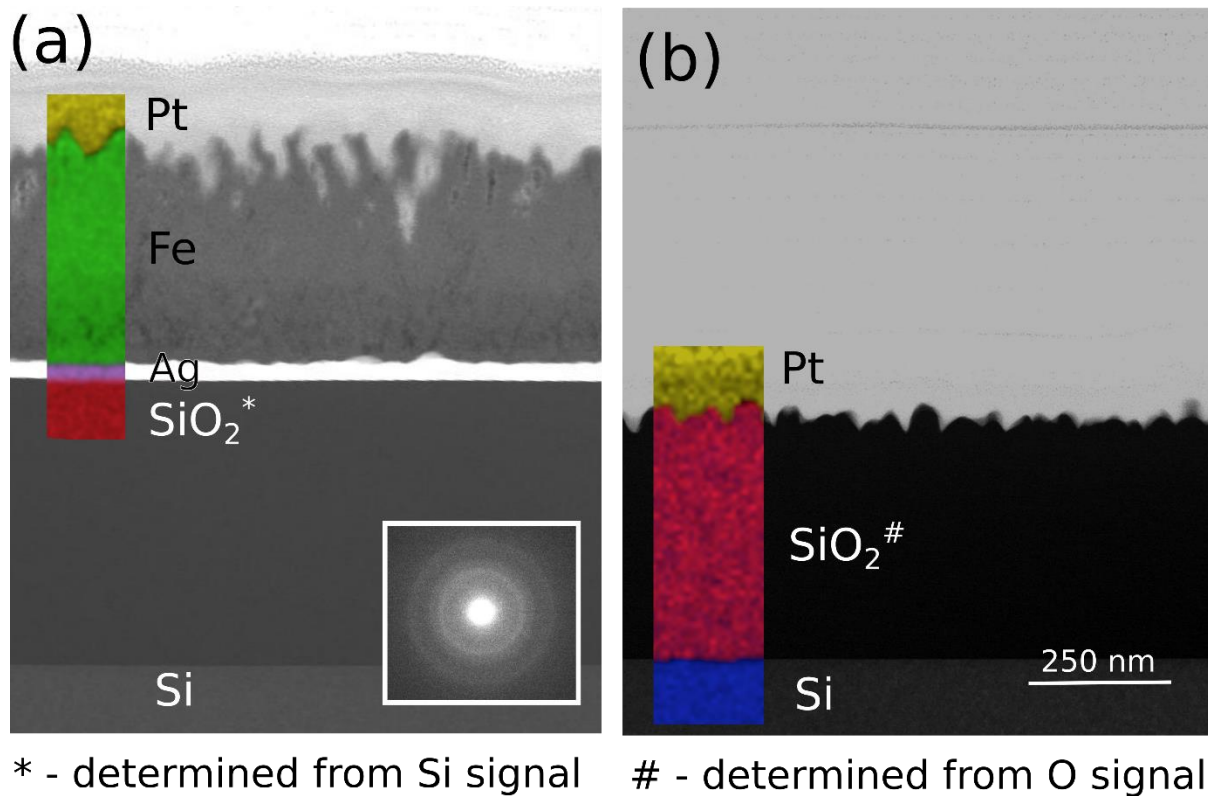


Figure 1: Cross sectional scanning transmission electron micrographs on the substrate regions with (a) and without (b) Ag coating: Insets show the compositional maps, which were derived directly from the STEM-EDS data. SAED of the deposited films are given as inserts.

High resolution XPS of the Fe spectral region recorded from the Si/SiO<sub>2</sub> substrate areas with and without Ag coating (Figure 2) show that the films deposited on the Ag coated areas consist of iron, confirming the EDS analysis (Figure 1). The XPS analysis show that the films deposited on the Ag coated areas are mixed iron oxides in the as-deposited, untreated, samples. The Fe 2p region (Figure 2a) shows peaks at 709.5–711.5 eV, corresponding to Fe–O.<sup>13</sup> It should be noted that these samples were subjected to air prior to being loaded into the XPS

chamber and given the oxyphilic nature of iron, surface oxidation is expected. Film deposition was also done in medium vacuum meaning that low levels of oxygen exposure is to be expected during the deposition.<sup>14</sup> The films were therefore sputter cleaned in the XPS chamber. After 1800 s sputtering, shoulder peaks at 706.9 and 720.1 eV ( $\Delta 13.2$  eV) corresponding to zero valent Fe  $2p_{3/2}$  and Fe  $2p_{1/2}$ ,<sup>13,15</sup> respectively can be seen (Figure 2a). After further sputtering to a total sputter time of 3000 s these peaks dominate the spectra. The composition analysis by XPS of sputtered clean films deposited on the Ag coated  $\text{SiO}_2$  shows 40 at. % Fe, 19.5 at. % C, 35 at. % O, 2.6 at. % N and 2.9 at. % Ti. In contrast, XPS analysis of the  $\text{Si}/\text{SiO}_2$  substrate areas not coated by Ag show very similar, albeit weaker, peaks, ascribed to iron oxides, in the as-deposited samples (Figure 2b). As these films were sputter cleaned for 1800 s, no change in peak position is observed and the peaks in the iron spectral region vanish after 3000 s sputtering on the  $\text{SiO}_2$  substrate, indicating a very thin iron oxide which could not be detected in the STEM analysis (Figure 1b). This shows that the amount of Fe deposited on the  $\text{SiO}_2$  substrate is very low compare to films deposited on the Ag coated part of the substrate.

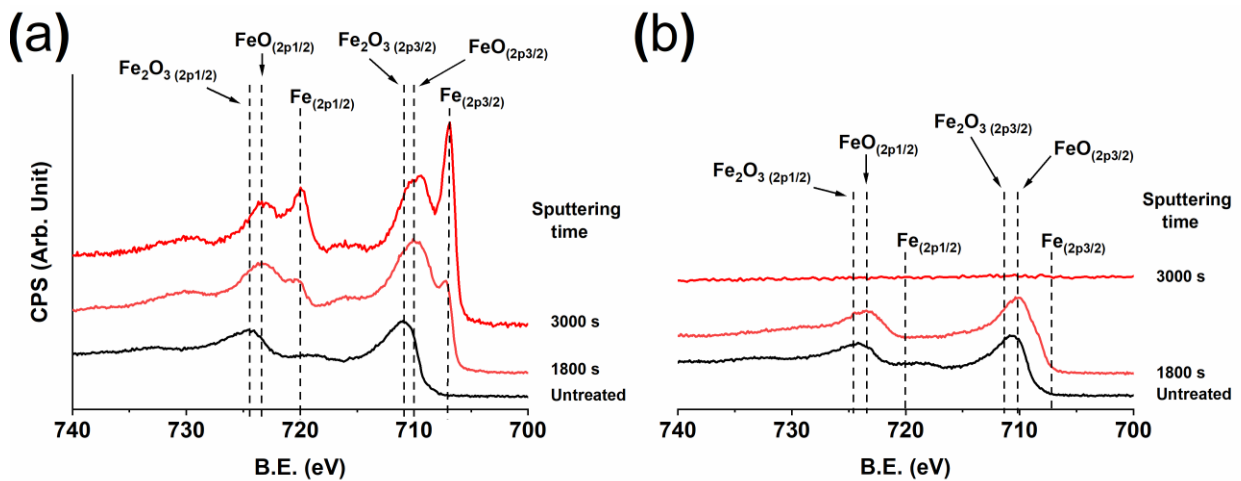


Figure 1. High resolution XPS spectra, showing the iron spectral region of deposited films on (a) the substrate regions with Ag coated  $\text{SiO}_2$  and (b) without Ag coated  $\text{SiO}_2$ .

Our experimental results suggest that the electrical resistivity of the surface determines the ability to deposit metallic films by this CVD method and that the CVD method is inherently area selective from the surface electrical resistivity. This inherent area selectivity of the new CVD process, where plasma electrons are used as reducing agents, does not depend on any thermodynamic or kinetic factors, as in other inherent ASD processes.<sup>16</sup> Instead, creating a low resistivity path for the electron flux from the plasma discharge to the substrate bias supply via the substrate surface is the prerequisite for the deposition chemistry in this new CVD process. We believe that this opens for exciting new possibilities for metal deposition selectively on metals.

## Notes

Henrik Pedersen and Hama Nadhom have filed a patent on the described CVD method.

## ACKNOWLEDGMENT

Michal Zanaska is acknowledged for assistance in sputtering the silver coating on the substrates. Financial support from the Swedish Research Council (VR) under Contracts 2015-03803 and 2019-05055 and from the Lam Research Corporation is gratefully acknowledged.

## REFERENCES

- (1) Carlsson, J.-O. Selective Vapor-Phase Deposition on Patterned Substrates. *Crit. Rev. Solid State Mater. Sci.* **1990**, *16* (3), 161–212.
- (2) Mackus, A. J. M.; Merkx, M. J. M.; Kessels, W. M. M. From the Bottom-Up: Toward Area-Selective Atomic Layer Deposition with High Selectivity. *Chem. Mater.* **2019**, *31*

- (1), 2–12.
- (3) Parsons, G. N.; Clark, R. D. Area-Selective Deposition: Fundamentals, Applications, and Future Outlook. *Chem. Mater.* **2020**, *32* (12), 4920–4953.
- (4) Minaye Hashemi, F. S.; Birchansky, B. R.; Bent, S. F. Selective Deposition of Dielectrics: Limits and Advantages of Alkanethiol Blocking Agents on Metal–Dielectric Patterns. *ACS Appl. Mater. Interfaces* **2016**, *8* (48), 33264–33272.
- (5) Kim, W.-H.; Minaye Hashemi, F. S.; Mackus, A. J. M.; Singh, J.; Kim, Y.; Bobb-Semple, D.; Fan, Y.; Kaufman-Osborn, T.; Godet, L.; Bent, S. F. A Process for Topographically Selective Deposition on 3D Nanostructures by Ion Implantation. *ACS Nano* **2016**, *10* (4), 4451–4458.
- (6) Kalanyan, B.; Lemaire, P. C.; Atanasov, S. E.; Ritz, M. J.; Parsons, G. N. Using Hydrogen To Expand the Inherent Substrate Selectivity Window During Tungsten Atomic Layer Deposition. *Chem. Mater.* **2016**, *28* (1), 117–126.
- (7) Mohimi, E.; Zhang, Z. V.; Liu, S.; Mallek, J. L.; Girolami, G. S.; Abelson, J. R. Area Selective CVD of Metallic Films from Molybdenum, Iron, and Ruthenium Carbonyl Precursors: Use of Ammonia to Inhibit Nucleation on Oxide Surfaces. *J. Vac. Sci. Technol. A* **2018**, *36* (4), 041507.
- (8) Kerrigan, M. M.; Klesko, J. P.; Rupich, S. M.; Dezelah, C. L.; Kanjolia, R. K.; Chabal, Y. J.; Winter, C. H. Substrate Selectivity in the Low Temperature Atomic Layer Deposition of Cobalt Metal Films from Bis(1,4-Di- Tert -Butyl-1,3-Diazadienyl)Cobalt and Formic Acid. *J. Chem. Phys.* **2017**, *146* (5), 052813.
- (9) Vos, M. F. J.; Chopra, S. N.; Verheijen, M. A.; Ekerdt, J. G.; Agarwal, S.; Kessels, W. M. M.; Mackus, A. J. M. Area-Selective Deposition of Ruthenium by Combining Atomic Layer Deposition and Selective Etching. *Chem. Mater.* **2019**, *31* (11), 3878–3882.



- (10) Nadhom, H.; Lundin, D.; Rouf, P.; Pedersen, H. Chemical Vapor Deposition of Metallic Films Using Plasma Electrons as Reducing Agents. *J. Vac. Sci. Technol. A* **2020**, *38* (3), 033402.
- (11) Langford, R. M.; Petford-Long, A. K. Preparation of Transmission Electron Microscopy Cross-Section Specimens Using Focused Ion Beam Milling. *J. Vac. Sci. Technol. A Vacuum, Surfaces, Film.* **2001**, *19* (5), 2186–2193.
- (12) Nordling, C.; Österman, J. Physics Handbook for Science and Engineering, 8<sup>th</sup> edition; Studentlitteratur: Lund, Sweden, 2006; pp 45-47.
- (13) Sault, A. G. Quantitative Analysis of Auger Lineshapes of Oxidized Iron. *Appl. Surf. Sci.* **1994**, *74* (3), 249–262.
- (14) Rayner, G. B.; O’Toole, N.; Shallenberger, J.; Johs, B. Ultrahigh Purity Conditions for Nitride Growth with Low Oxygen Content by Plasma-Enhanced Atomic Layer Deposition. *J. Vac. Sci. Technol. A* **2020**, *38* (6), 062408.
- (15) Peng, D. L.; Sumiyama, K.; Oku, M.; Konno, T. J.; Wagatsuma, K.; Suzuki, K. X-Ray Diffraction and X-Ray Photoelectron Spectra of Fe-Cr-N Films Deposited by DC Reactive Sputtering. *J. Mater. Sci.* **1999**, *34* (18), 4623–4628.
- (16) Cao, K.; Cai, J.; Chen, R. Inherently Selective Atomic Layer Deposition and Applications. *Chem. Mater.* **2020**, *32* (6), 2195–2207.

# TOC GRAPHICS

